available at www.sciencedirect.com

ScienceDirect

journal homepage: www.elsevier.com/locate/agrformet

Modelling energy and CO_2 fluxes with an interactive vegetation land surface model-Evaluation at high and middle latitudes

Anne-Laure Gibelin [a,*], *Jean-Christophe Calvet* [a], *Nicolas Viovy* [b]

[a] *Groupe d'Etude de l'Atmosphère Météorologique, Centre National de Recherches Météorologiques, Météo-France/CNRS, 42 Avenue Coriolis, F-31057 Toulouse Cedex 1, France*

[b] *Laboratoire des Sciences du Climat et de l'Environnement, Institut Pierre Simon Laplace, CEA/CNRS, Orme des Merisiers, F-91191 Gif sur Yvette, France*

ARTICLE INFO

Article history:
Received 20 November 2007
Received in revised form
14 May 2008
Accepted 15 May 2008

Keywords:
Carbon cycle
Carbon balance
Surface energy balance
Evapotranspiration
Eddy correlation

ABSTRACT

We developed ISBA-CC, a new version of the ISBA land surface model, to represent the fluxes and reservoirs of the terrestrial carbon cycle. The simulated latent heat flux, sensible heat flux and net ecosystem exchange are validated against in-situ measurements at 26 sites of the FLUXNET network, located at temperate and high latitudes of the Northern Hemisphere. Overall, ISBA-CC captures well the temporal variations of the fluxes, from the diurnal to the seasonal and the inter-annual scales. The best results are obtained for deciduous broadleaf and needle leaf forests, while the worst are found for agricultural sites, suggesting the need to take into account agricultural practices in order to better simulate both the energy fluxes and the net carbon flux. The ranking of the sites in terms of scores is consistent for the different fluxes. We show that taking into account the response of heterotrophic respiration to soil moisture allows a better representation of the variations of the net ecosystem exchange along with soil water content. ISBA-CC also compares favourably with other terrestrial ecosystem models. All these results show that the model matches the observed variability driven by the climate and can be used to assess the response of the terrestrial biosphere to future climate changes.

© 2008 Elsevier B.V. All rights reserved.

1. Introduction

Terrestrial ecosystems are a key component of the global carbon cycle. Carbon is stored in vegetation biomass, soil organisms and organic dead matter (about 2300 GtC, Sarmiento and Gruber, 2002). Large quantities of carbon are also exchanged between the terrestrial biosphere and the atmosphere. Atmospheric CO_2 is absorbed and fixed in the plant biomass by photosynthesis, while CO_2 is rejected by plant respiration and the dead biomass decomposition. The two main natural fluxes (gross primary production and ecosystem respiration) are estimated each at about 120 GtC year^{-1}, resulting in a nil net flux during the pre-industrial period (Sarmiento and Gruber, 2002). Since 1750, human activities (mainly fossil fuel burning and deforestation) have released large amounts of CO_2 into the atmosphere and have disrupted the natural carbon cycle. Overall, this perturbation enhances the uptake of carbon by the ecosystems, and about half of the anthropogenic CO_2 is absorbed by the terrestrial biosphere and the ocean, while the other part remains in the atmosphere (Ciais et al., 1995). Several processes, among which direct effects of increase in CO_2 on vegetation

* *Corresponding author*. Tel.: +33 5 61 07 96 35; fax: +33 5 61 07 96 10.
E-mail address: anne-laure.gibelin@meteo.fr (A.-L. Gibelin).
0168-1923/$ – see front matter © 2008 Elsevier B.V. All rights reserved.
doi:10.1016/j.agrformet.2008.05.013

physiology, namely CO_2 fertilization and increase in water use efficiency, explain the additional terrestrial sink. However, in the future decades, the oceanic and terrestrial sinks could decrease or even become carbon sources, because of climate changes resulting from the increase in atmospheric CO_2 concentration (Denman et al., 2007).

Numerical models are efficient tools to study and understand the carbon cycle in the past and to assess its evolution under future climate changes. Several modelling approaches have been developed to represent the terrestrial carbon cycle, depending on the main goal of the model. For example, existing models are classified in three approaches (biochemical, light-use efficiency and carbon assimilation) and two types (soil–vegetation–atmosphere transfer (SVAT) schemes and ecological models) by Arora (2002), depending on the method to estimate photosynthesis and the framework within which it is simulated. One of these approaches consists of adding biogeochemical processes to SVAT schemes, originally designed to provide surface energy and water fluxes to atmospheric models, in order to calculate consistent carbon and water exchanges between the terrestrial surface and the atmosphere (e.g. Foley et al., 1996; Sellers et al., 1996; Calvet et al., 1998; Cox et al., 1998; Dickinson et al., 1998; Krinner et al., 2005). In parallel, some models of oceanic carbon cycle have been developed, and these carbon cycle models can be coupled with general circulation models to investigate the interactions between the climate and the carbon cycle (e.g. Cox et al., 2000; Dufresne et al., 2002). Recently, Friedlingstein et al. (2006) inter-compared 11 coupled carbon-climate models driven by the Intergovernmental Panel on Climate Change (IPCC) Special Report on Emissions Scenarios (SRES) A2 emission scenario. All models simulated a positive feedback between the carbon cycle and the future climate for the end of the 21st century, i.e. an increase in both the atmospheric CO_2 concentration and in the global surface temperature. However, there was a large uncertainty on the magnitude of the feedback and on the relative sensitivities of the land and the ocean. Moreover, no consensus was found concerning the attribution of the reduction of land carbon absorption to changes in net primary production versus changes in respiration. These results show the need to improve the modelling of the carbon cycle in order to reduce the uncertainties in projections of future climate changes.

In this study, we present a new version of the SVAT-type ISBA model (Interactions between Soil, Biosphere and Atmosphere; Noilhan and Planton, 1989; Noilhan and Mahfouf, 1996), referred to as ISBA-CC (ISBA-Carbon Cycle), designed to simulate all the components of the terrestrial carbon cycle. ISBA-CC is based on the CO_2 reactive model ISBA-A-gs (Calvet et al., 1998). ISBA-A-gs simulates the carbon assimilation by photosynthesis (i.e. the gross primary production) and the evolution of the leaf biomass, but does not represent the other carbon reservoirs in the plant and in the soil. Moreover, the ecosystem respiration is parameterized by a very simple Q_{10} formulation only depending on soil temperature (Rivalland et al., 2005). This parameterization presents several limitations. First, no distinction is made between autotrophic and heterotrophic respiration, and the model is not able to calculate net primary production (NPP). Second, the parameterization requires to calibrate a respiration coefficient by using observations, but flux measurements are not available everywhere. Third, the effect of soil moisture on heterotrophic respiration is not taken into account. Finally, the parameterization does not simulate the carbon stored in the soil, and hence is not appropriate to study the evolution of the terrestrial carbon cycle over long periods of time. ISBA-CC was developed to overcome these flaws. ISBA-CC uses the same photosynthesis parameterization and leaf biomass growth model than ISBA-A-gs, which has been validated both in local and global studies (e.g. Calvet et al., 1998; Calvet and Soussana, 2001; Gibelin et al., 2006). We modified the growth model to represent all the biomass reservoirs in the plant (namely roots and woody biomass). This allowed to calculate the autotrophic respiration and to couple the model with a heterotrophic respiration module (Parton et al., 1987). Therefore, ISBA-CC is a state-of-the-art land surface model, able to simulate all the components of the terrestrial carbon cycle in a fully prognostic way. As mentioned before, there are large uncertainties in modelled land carbon fluxes. This new terrestrial ecosystem model will be helpful to explore these inter-model uncertainties, as it uses innovative formulations for photosynthesis (Jacobs et al., 1996) and its response to drought (Calvet, 2000; Calvet et al., 2004).

In this paper, we describe the new ISBA-CC model and validate it against flux measurements at 26 FLUXNET sites located at temperate and high latitudes of the Northern Hemisphere. We already compared the Leaf Area Index (LAI) simulated by ISBA-A-gs at global scale to satellite-derived estimates (Gibelin et al., 2006). It is essential to validate the carbon module at a finer temporal and spatial scale using direct in-situ measurements. The FLUXNET data set provides carbon and energy fluxes measured with the same method, which allows for a consistent validation of the respective simulated fluxes. With FLUXNET we can also analyze the performances of the model for various vegetation types and climate conditions. We focus on the model ability to reproduce both mean diurnal and seasonal cycles, as well as intra-seasonal and inter-annual variability, as these characteristics play a key role in the behaviour of the terrestrial biosphere as a sink or a source of carbon. They also permit an indirect validation of the prognostic vegetation phenology, which controls the partition of the net energy at the surface between the latent and the sensible heat flux, and the absorption of carbon by vegetation. We also pay attention to the variations of the carbon flux with soil moisture, as drought can limit both the carbon assimilation by photosynthesis and the carbon release by respiration. The FLUXNET data set is presented in Section 2. Section 3 presents the principles of the model (equations are fully described in Appendices A and B) and the simulations performed. Results concerning the validation of energy and carbon fluxes are presented and discussed in Section 4. ISBA-CC is also compared with the state-of-the-art model ORCHIDEE (Organizing Carbon and Hydrology in Dynamic EcosystEms, Krinner et al., 2005), which has been run for the same FLUXNET sites. Finally, Section 5 gives a summary of the results and future perspectives.

2. The FLUXNET data set

FLUXNET is a global cooperative network of tower sites designed to measure the exchanges between terrestrial

Table 1 – Characteristics of the 26 FLUXNET Sites

Code	Site name	Location	Selected years	ECOCLIMAP vegetation type	Citation
GU	Gunnarsholt	63°50′N 20°13′W	1996–1998	70% DBF and 30% CC3	Valentini et al. (2000)
HE	Hesse	48°40′N 7°04′E	1996–2000	DBF	Granier et al. (2000)
HV	Harvard Forest	42°32′N 72°11′W	1992–1999	70% DBF and 30% NLF	Goulden et al. (1996)
SO	Soroe	55°29′N 11°38′E	1997–1999	DBF	Pilegaard et al. (2001)
VI	Vielsalm	50°18′N 6°00′E	1996–1998	70% DBF and 30% NLF	Valentini et al. (2000)
WB	Walker Branch	35°57′N 84°17′W	1995–1998	80% DBF and 20% NLF	Wilson and Baldocchi (2000)
FL	Flakaliden	64°07′N 19°27′E	1996–1998	NLF	Lindroth et al. (1998)
HY	Hyytiälä	61°51′N 24°17′E	1996–2000	70% NLF and 30% CC3	Rannik et al. (2002)
NO	Norunda	60°05′N 16°13′E	1996–1998	NLF	Lindroth et al. (1998)
AB	Aberfeldy	56°36′N 3°48′E	1997–1998	90% NLF and 10% HC3	Valentini et al. (2000)
BR	Brasschaat	51°19′N 4°31′E	1996–1998	60% NLF and 40% DBF	Carrara et al. (2003)
BX	Bordeaux	44°43′N 0°46′W	1997–1998	70% NLF and 30% HC3	Berbigier et al. (2001)
LO	Loobos	52°10′N 5°44′E	1996–2000	80% NLF and 20% HC3	Dolman et al. (2002)
ME	Metolius	44°27′N 121°33′W	1996–1997	NLF	Law et al. (2001)
TH	Tharandt	50°58′N 13°34′E	1996–2000	80% NLF and 20% HC3	Valentini et al. (2000)
WE	Weiden Brunnen	50°10′N 11°53′E	1996–1999	80% NLF and 20% HC3	Valentini et al. (2000)
SKo	Sky Oaks (old stand)	33°22′N 116°37′W	1997–2000	80% EBF and 20% HC4	Law et al. (2002)
SKy	Sky Oaks (young stand)	33°22′N 116°37′W	1997–2000	80% EBF and 20% HC4	Law et al. (2002)
CP	Castelporziano	41°45′N 12°22′E	1997–1998	70% EBF and 30% bare soil	Valentini et al. (2000)
PO	Ponca City	36°46′N 97°08′W	1997	CC3	Law et al. (2002)
BVS	Bondville	40°00′N 88°18′W	1998	CC3	Meyers (2001)
BVC	Bondville	40°00′N 88°18′W	1997 and 1999	CC4	Meyers (2001)
UP	Upad	70°16′N 148°53′W	1994	50% HC3 and 50% bare soil	Oechel et al. (2000)
LW	Little Washita	34°57′N 97°59′W	1997–1998	HC4	Meyers (2001)
FI	FIFE	39°07′N 95°29′W	1987	HC4	Betts and Ball (1998)
SH	Shidler	36°56′N 96°41′W	1997	HC4	Law et al. (2002)

Abbreviations for the ECOCLIMAP vegetation types are DBF: deciduous broadleaf forests; EBF: evergreen broadleaf forests; NLF: needle leaf forests; HC3: C_3 natural herbaceous; HC4: C_4 natural herbaceous; CC3: C_3 crops; CC4: C_4 crops.

ecosystems and the atmosphere (Baldocchi et al., 2001). FLUXNET offers a unique data set to validate land surface models, as it operates on a long-term and a continuous basis, and it samples the main biomes worldwide. In this study, we used a set of 25 sites (Falge et al., 2005) located at high and temperate latitudes of the Northern Hemisphere, listed in Table 1. In addition, we also used the 1987 FIFE site-average dataset collected over a prairie of central Kansas (Betts and Ball, 1998). For convenience, these 26 sites are designated as FLUXNET sites everywhere else in this paper. All these sites were selected by Krinner et al. (2005) to validate the ORCHIDEE model, according to the availability of meteorological forcing and quality criteria on measurements.

Exchanges of carbon dioxide (CO_2), water vapour and energy are measured above the vegetation canopy using eddy covariance methods. We used available half-hourly fluxes to evaluate the latent heat flux, the sensible heat flux and the net carbon ecosystem exchange simulated by ISBA-CC. The FLUXNET data set also provides all the meteorological variables necessary to force a land surface model: downward solar radiation, downward infrared radiation, air temperature, air humidity, precipitation, wind speed, and surface pressure. Long-term model simulations need continuous temporal climate series, and missing data were reconstructed using the gap-filling method described in details by Krinner et al. (2005). Nearby weather stations provided average, minimum, and maximum daily temperature, mean daily dew point temperature, daily precipitation, and mean daily wind speed. A linear regression was then applied to calculate the daily average at the FLUXNET site, except for rainfall. The ECMWF ERA15 1×1 degree reanalysis was used to get the incoming short-wave radiation. Half-hourly values were rebuilt from the daily averages by applying a shape of diurnal cycle depending on the variable. The incoming long-wave radiation was computed from air temperature, air humidity, and incoming short-wave radiation. For surface air pressure, gaps were filled with the average value at the site if measurements were available, otherwise a constant value of 1015 hPa was taken. Moreover, ISBA-CC needs distinct liquid and solid precipitation to resolve the energy and the water balance. Total precipitation was split into snowfall and rainfall linearly according to the air temperature between $-2\,^{\circ}C$ and $0\,^{\circ}C$. Beyond these values, precipitation was totally converted into either snow or rain, respectively. Finally, each forcing variable was interpolated at the 5 mn time step of the model.

3. Modelling

The ISBA model (Interactions between Soil, Biosphere and Atmosphere) (Noilhan and Planton, 1989; Noilhan and Mahfouf, 1996) is a land surface model designed to calculate the exchanges of water and energy between the land surface and the atmosphere, for use in numerical weather prediction models and climate models. A CO_2-responsive version of ISBA, called ISBA-A-gs (Calvet et al., 1998), allows accounting for the effect of the atmospheric carbon dioxide concentration and the interactions between all environmental factors on the stomatal aperture. ISBA-A-gs also calculates the two main carbon fluxes between the land surface and the atmosphere (i.e. gross primary production and total ecosystem respiration). In this study, we developed a new version of ISBA,

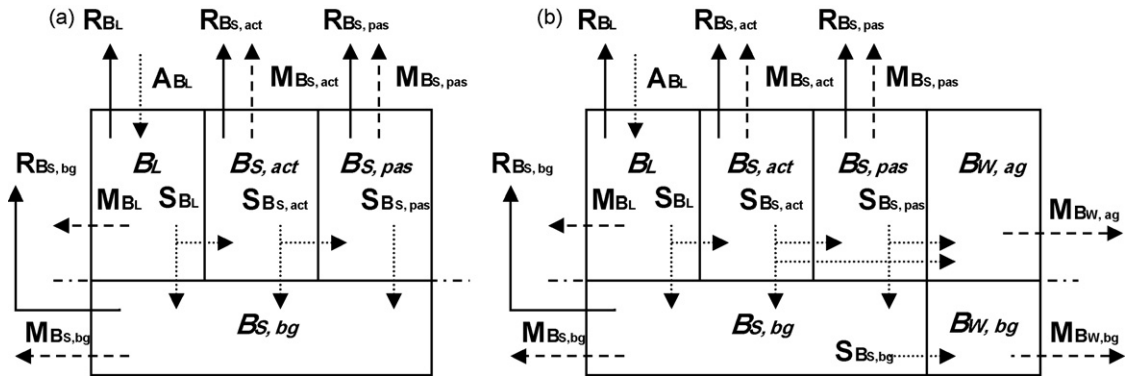

Fig. 1 – Schematic representation of the plant carbon reservoirs and fluxes in ISBA-CC for herbaceous (a) and woody (b) vegetation. The various biomass reservoirs (prefixed by B) are listed in Table 2. Input and output fluxes are indicated for each reservoir (see Appendix A for details): allocation and storage (A and S, dotted arrows), mortality (M, dashed arrows) and respiration (R, solid arrows). The autotrophic respiration is the sum of all the biomass respiration terms.

named ISBA-CC (ISBA-Carbon Cycle), in order to represent in a more detailed manner the fluxes and the reservoirs of the terrestrial carbon cycle.

3.1. *Photosynthesis*

ISBA-CC uses the parameterization of photosynthesis of ISBA-A-gs, based on the model of Goudriaan et al. (1985) modified by Jacobs et al. (1996). This parameterization is different from that commonly used in most land surface models (Farquhar et al., 1980 for C_3 plants and Collatz et al., 1992 for C_4 plants). Farquhar's model aims to describe biochemical processes of photosynthesis, while Jacobs' one is based on the concept of resistance to diffusion of CO_2, analogous to that used in some parameterizations of physical processes in atmospheric models. The model calculates successive limitations of photosynthesis rate by temperature, atmospheric CO_2 concentration, air humidity, and light intensity. It has the same formulation for C_4 plants as for C_3 plants differing only by the input parameters. The model also includes an original representation of the soil moisture stress. Two different types of drought responses are distinguished for both herbaceous vegetation (Calvet, 2000) and forests (Calvet et al., 2004), depending on the evolution of the water use efficiency (WUE) under moderate stress: WUE increases in the early soil water stress stages in the case of the drought-avoiding response, whereas WUE decreases or remains stable in the case of the drought-tolerant response.

3.2. *Carbon allocation and autotrophic respiration*

ISBA-A-gs calculates interactively the leaf biomass and the Leaf Area Index (LAI) (defined as the leaf area per unit ground area), using a simple growth model (Calvet et al., 1998). The leaf biomass is supplied with the carbon assimilated by photosynthesis, and decreased by a turnover and a respiration terms. Phenology is modelled implicitly: LAI is inferred from the leaf biomass multiplied by the Specific Leaf Area (SLA) ratio, which depends on the leaf nitrogen concentration (Calvet and Soussana, 2001; Gibelin et al., 2006). SLA is calculated from vegetation parameters listed in Table 4: $SLA = e\ N_l + f$. Gibelin et al. (2006) showed that ISBA-A-gs simulates realistic LAI at the global scale under various environmental conditions, and this growth model therefore remains unchanged in ISBA-CC. The growth model has been completed by adding new biomass reservoirs in order to represent all the living carbon in the plant. A schematic representation of the growth model is shown in Fig. 1. ISBA-CC simulates 4 (6) biomass reservoirs in all for herbaceous (woody) vegetation types (Table 2). Leaf biomass B_L and active structural biomass $B_{s,act}$ correspond to metabolic biomass B and structural biomass B_s respectively, previously defined by Calvet and Soussana (2001) and related by the nitrogen decline equation. The passive structural biomass $B_{s,pas}$ is a part of B_{s2} in Calvet and Soussana (2001), and the sum of structural reservoirs ($B_{s,act} + B_{s,pas}$) represents the non-woody above ground biomass different from leaves. Roots are now explicitly represented, with a non-woody below ground biomass ($B_{s,bg}$). Moreover, two woody reservoirs $B_{w,ag}$ and $B_{w,bg}$ (above and below ground) are now simulated for woody vegetation.

The variation of each biomass reservoir during one day is calculated according to the generic Eq. (1):

$$\frac{\Delta B}{\Delta t} = A_B - D_B - R_B \tag{1}$$

where B (kg m^{-2}) is one of the biomass reservoir listed in Table 2, $\Delta t = 1$ day, A_B (kg m^{-2} day^{-1}) is a term of increase in biomass coming from photosynthetic assimilation or allocation from another reservoir, D_B (kg m^{-2} day^{-1}) is a decrease term due to mortality (M_B) or reallocation to another reservoir

Table 2 – List of the plant biomass reservoirs simulated by ISBA-CC

B_L	Leaf biomass
$B_{s,act}$	Active structural biomass
$B_{s,pas}$	Passive structural biomass
$B_{s,bg}$	Below ground structural biomass
$B_{w,ag}$	Above ground woody biomass
$B_{w,bg}$	Below ground woody biomass

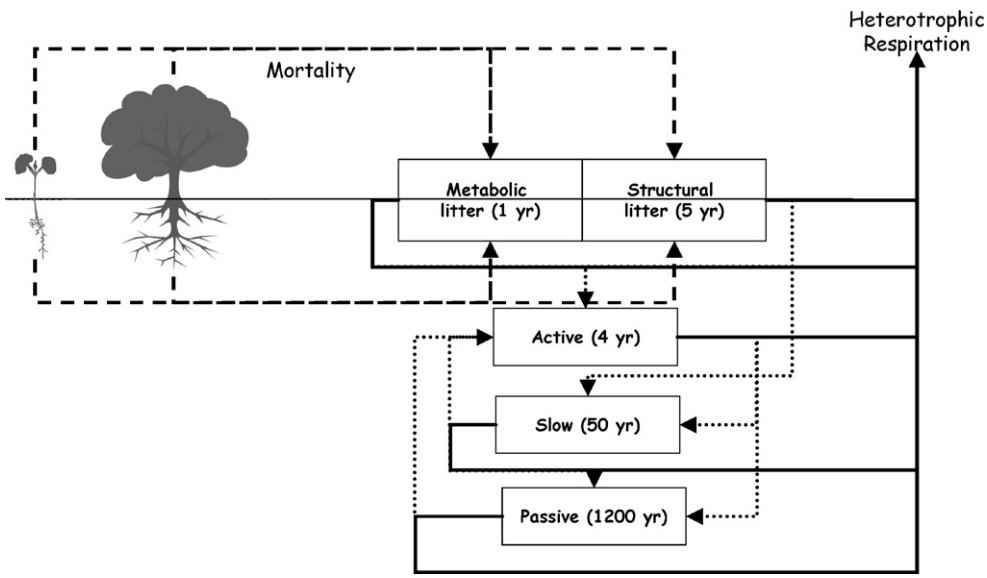

Fig. 2 – Schematic representation of the heterotrophic respiration parameterization of ISBA-CC, adapted from Parton et al. (1987). The soil carbon pools are indicated together with input mortality terms (dashed lines), fluxes of carbon exchanged between the pools (dotted lines), and fluxes of mineralized carbon (solid lines). The heterotrophic respiration is the sum of all the fluxes of mineralized carbon.

(S_B), and R_B (kg m^{-2} day^{-1}) is a decrease term due to respiration. All of these terms are explicitly described for each reservoir in Appendix A.

The autotrophic respiration R_a (gC m^{-2} day^{-1}) is the sum of all the respiration terms of the plant (there is no respiration term associated to woody reservoirs):

$$R_a = 10^3 P_C (R_{B_L} + R_{B_{s,act}} + R_{B_{s,pas}} + R_{B_{s,bg}}) \quad (2)$$

where P_C is the proportion of carbon in the dry plant biomass (a value of P_c = 40% is used as in Calvet et al., 1998).

3.3. *Heterotrophic respiration*

ISBA-CC also includes a parameterization of heterotrophic respiration following Parton et al. (1987), schematized in Fig. 2. The model simulates seven soil organic matter pools in all, listed in Table 3. Four litter pools are differentiated, depending on the lignin content of the input residues (metabolic litter for low lignin content or structural litter for high lignin content) and their location (above- or below-ground). The litter pools are supplied by the fluxes of dead biomass M_B from each biomass reservoir (see Appendix A). The model also simulates three soil carbon pools (active, slow and passive). They are characterized by their turnover times (from a few years for the active pool to 1200 years for the passive pool). The various pools represent different states of resistance to the decomposition of organic matter, but the vertical distribution of carbon is not dealt with. The model calculates the evolution of the seven carbon pools due to the decomposition of the organic matter, and the fluxes of carbon exchanged between the pools and rejected into the atmosphere. The equations of the soil carbon model are fully described in Appendix B.

Table 3 – List of the soil organic matter pools simulated by ISBA-CC

$LC_{s,ag}$	Above ground structural litter
$LC_{m,ag}$	Above ground metabolic litter
$LC_{s,bg}$	Below ground structural litter
$LC_{m,bg}$	Belohw ground metabolic litter
SC_{act}	Active soil carbon
SC_{slow}	Slow soil carbon
SC_{pas}	Passive soil carbon

The heterotrophic respiration R_h (gC m^{-2} day^{-1}) is the sum of the mineralized carbon fluxes produced by decomposition in all carbon pools during one day:

$$R_h = \sum_C f_{C,CO_2} \frac{dC}{dt} \quad (3)$$

where f_{C,CO_2} is the fraction of the decomposition flux dC/dt from the carbon pool C that is mineralized (see Appendix B).

3.4. *Simulations*

ISBA-CC is run off-line at the 26 FLUXNET sites of Table 1, in the tile version to deal with the surface heterogeneity: the simulation is performed for each vegetation type present at the site, and then the fluxes are averaged weighted by the fraction of each type. At the scale representative of a FLUXNET site, soil carbon is a mix of inputs from all vegetation types. The assumption that vegetation types are separated is realistic at the larger spatial scales usually simulated by land surface models. In this case, it is essential to simulate separately the evolution of soil variables for each type (in particular for soil moisture which highly varies spatially), as some surface parameters of the model strongly depend on the vegetation type, e.g. root depth. Moreover, the simulation of soil carbon pools has to be consistent with the other soil variables

Table 4 – Values of ISBA-CC parameters for the ECOCLIMAP vegetation types (g_m^* in mm s^{-1}; τ_M in days; τ_w in years; LAI$_{min}$ in m^2 m^{-2}; D_{max}^* in g kg^{-1}; f_0^* dimensionless; g_c in mm s^{-1}; strategy of response to soil moisture stress (drought-tolerant or drought-avoiding), θ_C dimensionless; e in m^2 kg^{-1} %$^{-1}$; f in m^2 kg^{-1}; and N_l in %)

Vegetation type	g_m^*	τ_M	τ_w	LAI$_{min}$	D_{max}^*	f_0^*	g_c	Strategy	θ_C	e	f	N_l
Deciduous broadleaf trees	3	230	40	0.3	109	0.51	0.15	Tolerant	0.3	4.83	2.53	2
Evergreen broadleaf trees	2	365	30	1	124	0.57	0.15	Tolerant	0.3	4.83	2.53	2.5
Needle leaf trees	2	365	50	1	124	0.57	0	Avoiding	0.3	4.85	−0.24	2.8
C_3 crops	1	150	–	0.3	50	0.95	0.25	Avoiding	0.3	3.79	9.84	1.3
C_4 crops	9	150	–	0.3	33	0.6	0.15	Tolerant	0.3	7.68	−4.33	1.9
C_3 natural herbaceous	1	150	–	0.3	50	0.95	0.25	Tolerant	0.3	5.56	6.73	1.3
C_4 natural herbaceous	6	150	–	0.3	52	0.6	0.15	Tolerant	0.3	7.68	−4.33	1.3

(temperature and soil water content) that play a role in their evolution. The surface parameters (such as soil texture, albedo, emissivity, surface roughness and parameters listed in Table 4) are prescribed from ECOCLIMAP, a global database of surface parameters providing a coherent ensemble of the soil and vegetation characteristics used to initialize the land surface models (Masson et al., 2003). The model parameters are the same as those used in two dimensions simulations so that the main conclusions of our validation study remain valid at a larger scale. The values of the vegetation parameters specific to ISBA-A-gs are the same as those used at the global scale by Gibelin et al. (2006) (Table 4). The unstressed mesophyll conductance at 25 °C, g_m^*, controls the carbon assimilation in the model of photosynthesis. The potential leaf life expectancy τ_M controls the turnover rates of the leaf and the structural biomass pools, while τ_w controls the turnover rates of woody reservoirs. A minimum LAI value, LAI$_{min}$, is needed to calculate a minimum level of photosynthesis at the start of the growing season. D_{max}^* is the maximum leaf-to-air saturation deficit, i.e. the value of deficit above which stomata are fully closed. f_0^* is the maximum ratio between the intercellular and the atmospheric CO_2 concentration, reached when the deficit is 0. The cuticular conductance g_c describes the diffusion of water and carbon through the cuticle. Two different types of drought responses are distinguished for both herbaceous vegetation (Calvet, 2000) and forests (Calvet et al., 2004), depending on the evolution of the water use efficiency (WUE) under moderate stress: in the case of the drought-avoiding response, the WUE increases in response to a moderate soil water stress, whereas in the case of the drought-tolerant response, the WUE decreases or remains stable. The choice of the strategy of response to soil water stress is derived from previous studies at the local scale (Calvet, 2000; Calvet et al., 2004; Rivalland et al., 2005; Calvet et al., 2007): the drought-avoiding strategy is adopted for needle leaf forests and C_3 crops, while the drought-tolerant strategy is selected for deciduous and evergreen broadleaf forests, C_4 crops and C_3 and C_4 natural grasslands. Residence time of the woody biomass is adapted from Krinner et al. (2005), depending on the vegetation type. The critical extractable soil moisture θ_c is a threshold used for the parameterization of response to soil water stress. The nitrogen plasticity parameters e and f and the foliar nitrogen concentration N_l are used to calculate the ratio between LAI and leaf biomass. The atmospheric CO_2 concentration is kept constant and set equal to 350 ppm.

ISBA-CC is run with a 5 mn time step. The original soil carbon model CENTURY was designed for a use with a monthly time step (Parton et al., 1987), but here the heterotrophic respiration parameterization is used with the model time step to be consistent with the other parameterizations of the land surface model, and avoid large discontinuities in heterotrophic respiration.

The biomass reservoirs and the soil carbon pools simulated by ISBA-CC are not measured at FLUXNET sites and cannot be initialized realistically. Therefore, three spin up simulations are run to reach the equilibrium of all the reservoirs: the first one (10 years) for fast reservoirs such as soil water content or leaf biomass, the second one (500 years) for woody biomass reservoirs, and the third one (10 000 years) for the soil carbon pools. After each of these two last simulations, a supplementary 10-years spin up simulation is run to ensure the equilibrium of fast reservoirs. After that, the final simulation is performed during the period of available meteorological forcing for each site (see Table 1). This procedure involves that the gross primary production simulated by the model is balanced by the ecosystem respiration and that the net ecosystem exchange flux is close to zero, on an annual basis. Yet, most of the FLUXNET sites of this study are carbon sinks (Law et al., 2002). At this spatial scale, the behaviour of the terrestrial biosphere as a sink or a source is driven by climate and CO_2 concentration, but also by natural disturbances and anthropogenic management. Due to the lack of information about some of these factors, predicting the real value of the carbon budget was not feasible. Therefore, there is a systematic bias in the simulation which is not due to the model but to the insufficient knowledge of the history of the site, and a direct comparison of the absolute net carbon exchange simulated by the model with the observations is not possible. Since we assumed that the difference is related to the impossibility to initialize the soil and the vegetation carbon stocks, we corrected the ecosystem respiration without changing the gross primary production. Thus, the simulated NEE is corrected to obtain the same mean value as the observed NEE over the simulation period, by scaling the modelled ecosystem respiration by a constant factor. For that reason, only the temporal variations of NEE are considered in the following.

4. Results and discussion

4.1. *Energy fluxes*

In this study, we evaluate the ability of the model to represent both the seasonal and the diurnal variations of the exchanges between the terrestrial surface and the atmosphere. Contrary

Table 5 – Mean values (calculated with all dates for which measurements are available) of observed and modelled fluxes, and RMSE between monthly means for net radiation (Rnet), latent heat flux (LE) and sensible heat flux (*H*) (W m^{-2}) at the 26 FLUXNET sites

Code	Observed Rnet	Modelled Rnet	RMSE Rnet	Observed LE	Modelled LE	RMSE LE	Observed *H*	Modelled *H*	RMSE *H*
GU	47	62	18	20	25	8	−7	37	47
HE	75	73	15	34	40	12	6	32	30
HV	76	97	25	38	35	18	34	65	43
SO	–	–	–	20	28	12	11	22	24
VI	64	54	19	22	24	7	24	48	30
WB	95	133	41	48	73	29	34	73	45
FL	53	41	27	20	19	11	10	24	33
HY	68	58	32	23	27	11	16	20	22
NO	55	66	17	29	27	8	15	48	43
AB	53	59	19	16	20	10	7	41	39
BR	61	72	18	22	28	11	4	35	37
BX	97	88	11	50	46	13	21	51	32
LO	62	64	10	39	25	17	8	39	33
ME	98	142	55	42	30	16	43	130	93
TH	60	70	17	36	41	16	26	28	17
WE	68	60	24	29	38	17	0	34	41
SKo	123	133	45	48	45	38	100	124	45
SKy	118	144	50	28	49	38	89	108	46
CP	118	85	34	34	33	14	44	57	23
PO	87	133	47	65	84	46	22	52	43
BVS	83	106	25	50	62	40	21	44	41
BVC	84	105	33	46	50	18	29	55	32
UP	105	112	23	43	32	18	45	55	32
LW	103	125	25	37	54	28	42	77	39
FI	–	–	–	106	103	13	24	30	20
SH	109	125	22	47	71	36	24	54	36

to meteorological forcing, gap filling of observed fluxes is not necessary to compare the model to the observations. Thus, the comparison was done by selecting only the model values for dates when observations are available. For the annual cycle validation, in-situ observations and model outputs are first averaged monthly. Then, statistics (correlation coefficients and root mean square errors) are calculated by considering only the months for which more than half of measurements are present. For the diurnal cycle validation, model outputs are averaged half-hourly, and statistics are calculated with June, July and August (JJA) time series, when the surface fluxes are the largest. Anomalies series are calculated by subtracting the mean annual cycle (at a monthly time step) and the mean summer daily cycle (at a half-hourly time step) from monthly means and half-hourly values, respectively. The correlation coefficients between the monthly anomalies and between half-hourly anomalies allow assessing the performance of the model to capture inter-annual and intra-seasonal variability, respectively.

Table 5 shows the mean observed and modelled values, as well as root mean square errors (RMSE), for net radiation (Rnet), latent heat flux (LE) and sensible heat flux (*H*) at the 26 FLUXNET sites. The difference between model and observations is generally less than 25 W m^{-2} for Rnet, except for sites WB, ME, SKy, CP and PO. These highest values are due to an over-estimation of the energy absorbed by the surface, except for CP. For LE, the bias is generally lower than 15 W m^{-2}, and the largest differences with observations are due to an over-estimation of the flux by the model during the peak in spring and summer. The differences are larger for *H* and correspond to a systematic positive bias of the model for all sites. RMSEs are of same order of magnitude as biases. Fig. 3 shows examples of observed and modelled mean annual cycles for LE, H and NEE for a deciduous forest site (HE), a coniferous site (BX), an agricultural site (PO) and a natural herbaceous site (LW). The model reproduces well the amplitude of the latent heat flux for HE and BX, but underestimates LE for PO and LW. The sensible heat flux is underestimated for all sites, but the annual dynamics is realistic. Besides, the phasing of the cycles is generally captured well by the model for the three fluxes, both for the peak and the beginning and the end of the cycle. As a result of the larger bias for *H* than for LE, the model shows a lot of sites with a larger *H* than LE, whereas most sites have a larger mean LE in observations (Fig. 4). However, the model is able to reproduce the main outliers with a very large *H* (SKo and SKy) or LE (FI), as well as the relative position of sites within a vegetation type, in particular for deciduous broadleaf forests, C_3 crops and C_4 natural herbaceous (Table 5 and Fig. 4). Such differences between the model and the observations may look huge, but the eddy correlation method is associated with several limitations, due for example to sampling duration and frequency, instruments drift and calibration, or validity of steady-state conditions and constant flux layer assumptions (Baldocchi et al., 2001). As a result, flux measurements often reveal a lack of closure of the surface energy balance (Twine et al., 2000; Wilson et al., 2002). Wilson et al. (2002) found a mean imbalance in the order of 20% for 22 FLUXNET sites, 16 of which are used in this study, due to an under-estimation of the sum of the turbulent energy fluxes (LE + *H*) compared to the available energy. Such an imbalance prevents validation of the absolute values of the modelled fluxes, and in the following we focus only on the temporal variations of the fluxes at various

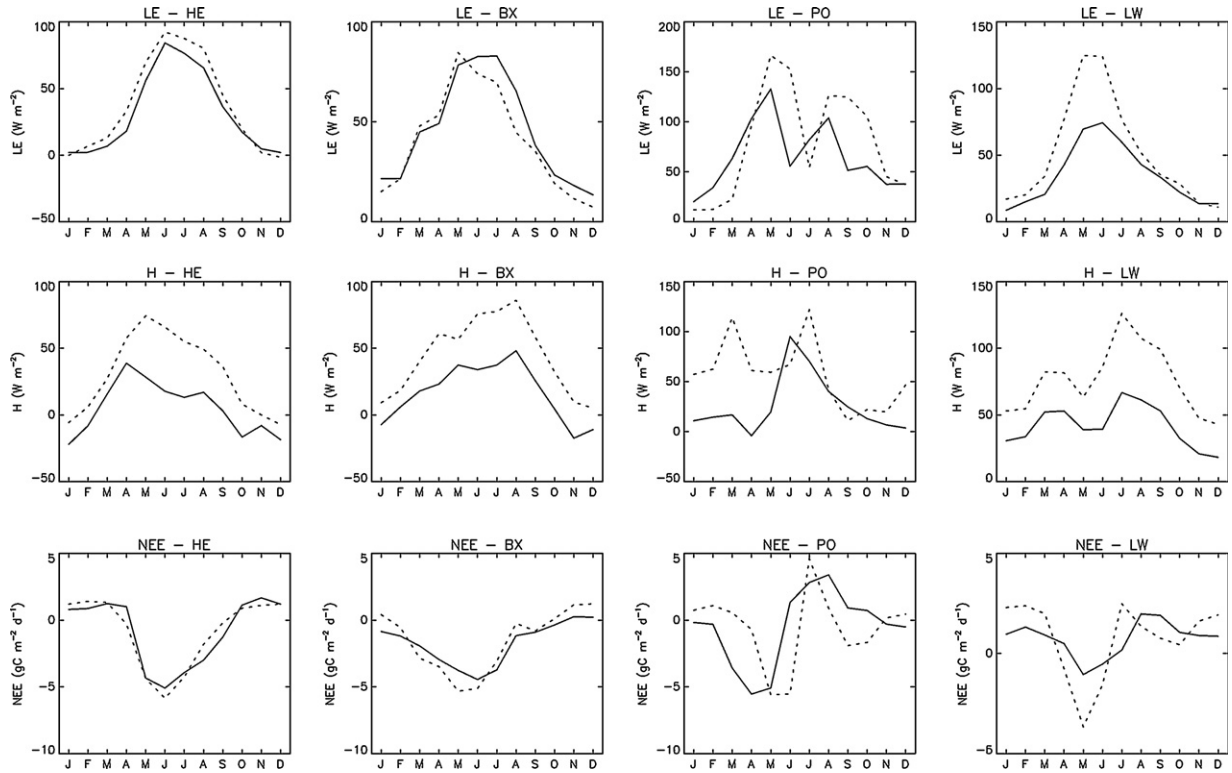

Fig. 3 – Mean annual cycle of LE (a), H (b) and NEE (c) at a deciduous forest site (HE), a coniferous forest site (BX), an agricultural site (PO) and a natural herbaceous site (LW): observations (solid line) and model (dashed line).

time scales (Figs. 5 and 6). Correlations between LE monthly means are generally higher than 0.8 (except for HV, ME, SKo, SKy, PO and UP), showing a good representation of the annual cycle by the model. Variations of *H* also generally agree with observations, but poor correlations are obtained for PO, BVS, UP and FI (Fig. 5a). For sites where several years of data are available, correlations between deseasonalized monthly anomalies show that the model is able to represent well the inter-annual variability for some sites (e.g. HE, WB, LO, SKy, BVC), but also obtains very low scores for some other sites (HV, AB, CP) (Fig. 5b). Diurnal statistics are less sparse but correlation of *H* is still very low for the BVS site, and intra-seasonal variations of LE or *H* are not reproduced well for ME, CP, BVS and FI (Fig. 6).

The largest differences between modelled and observed heat fluxes are obtained for sites where the net radiation is also badly reproduced (WB, ME, SKo, SKy, PO and BVS). Differences between the model and the observations can be attributed to three main sources of errors: errors in the atmospheric forcing, errors in the model and errors in the flux

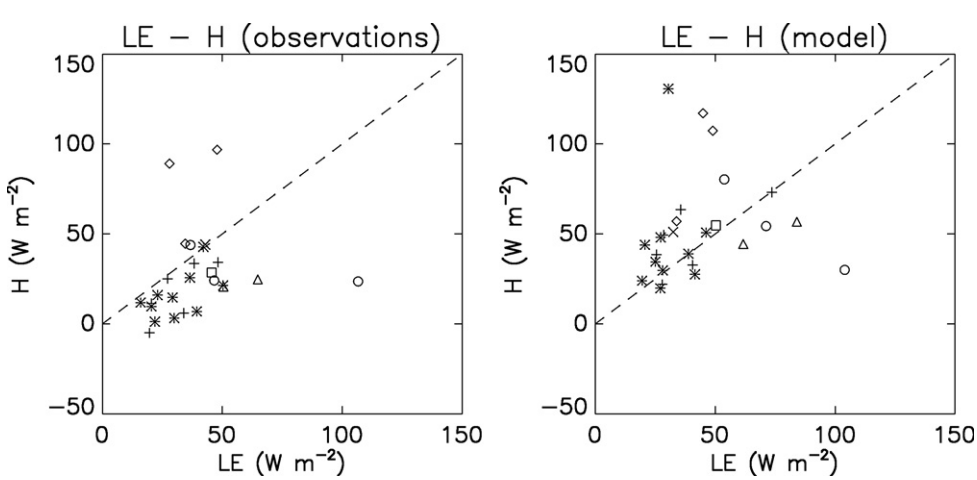

Fig. 4 – Mean annual values of latent heat flux (LE) and sensible heat flux (*H*) at the 26 FLUXNET sites for measurements (a) and ISBA-CC (b). Each symbol corresponds to one vegetation type: DBF (plus signs), EBF (diamonds), NLF (asterisks), HC3 (× signs), HC4 (circles), CC3 (triangles) and CC4 (squares).

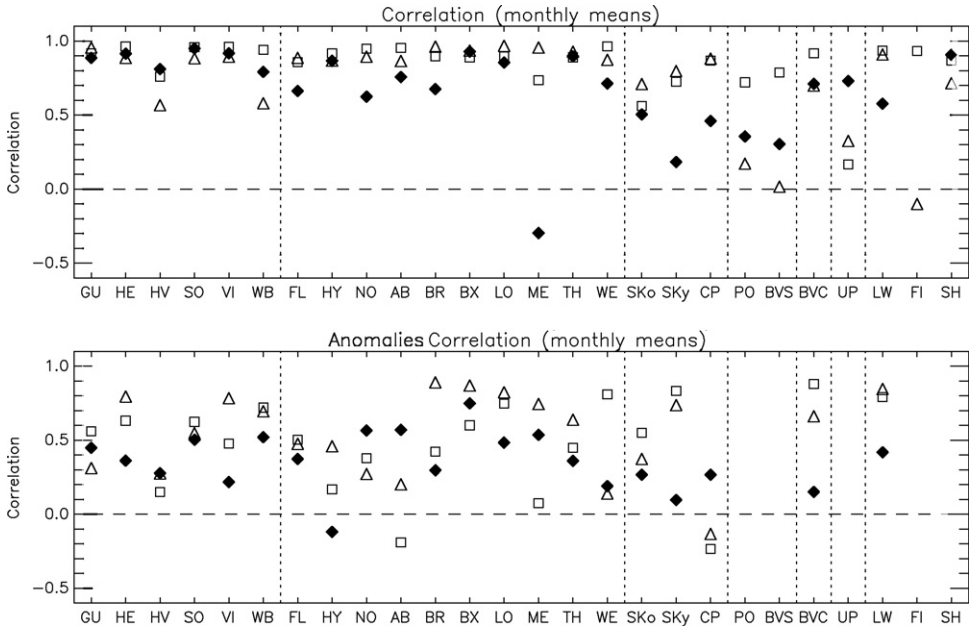

Fig. 5 – Correlation coefficients between the monthly means (a) and the deseasonalized monthly means (b) of the fluxes simulated by ISBA-CC and measured at FLUXNET sites (open squares: LE; open triangles: H; solid diamonds: NEE). Vegetation types are divided by vertical lines, from left to right: DBF, NLF, EBF, CC3, CC4, HC3, HC4.

measurements. As there are missing values in measurements, the atmospheric variables series have been gap-filled, and that can be a first source of uncertainty. Solar downward radiation in particular was reconstructed from the climatology of the ERA-15 reanalysis, but simulated radiation of ERA-15 at 1° resolution can differ largely from in-situ radiation. Moreover no inter-annual variation in solar downward radiation was taken into account. Likewise, long-wave radiation was retrieved from air temperature, air humidity and solar radiation. Differences can also come from the model formulation and the choice of parameters values. For example, the surface albedo controls the net radiation. It can be underestimated if the bare soil fraction is too low in the model. In the absence of a detailed description of the actual vegetation cover and to be consistent with the formulation of the model at any horizontal scale, the vegetation fraction is defined empirically as a constant for forests in this study, and its relatively high value (0.95 for needle leaf forests and deciduous broadleaf forests, and 0.99 for evergreen broadleaf forests) can explain the over-estimation of the net radiation for WB, ME, SKo and SKy. On the contrary, CP is the only site for which a large fraction of bare soil is imposed (30%) and where the model

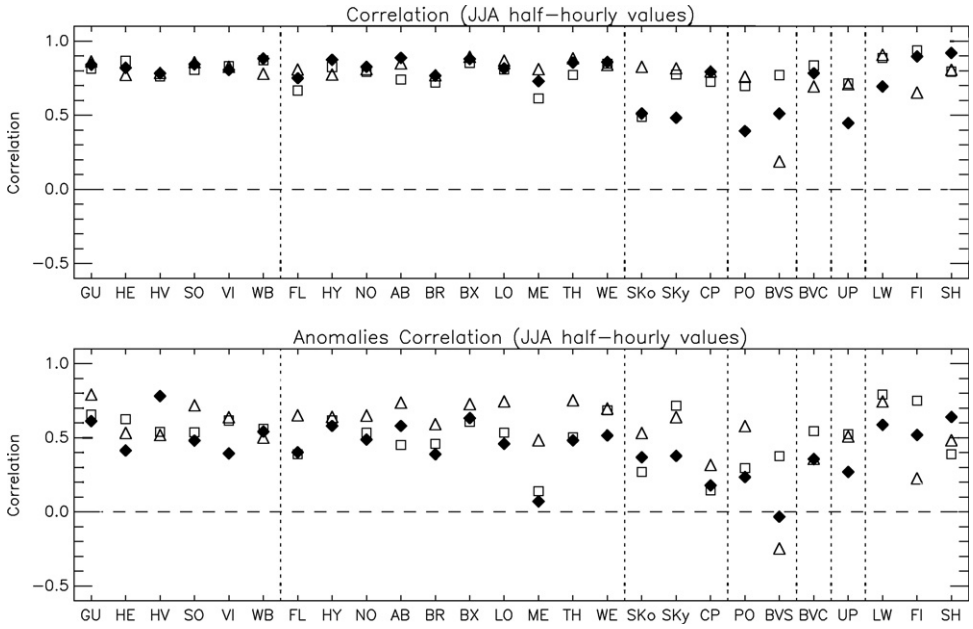

Fig. 6 – Same as Fig. 5 but for JJA half-hourly values (a) and JJA half-hourly anomalies to the mean diurnal cycle (b).

under-estimates the net radiation. Moreover, key model variables, like soil water content or LAI, drive the partitioning of net radiation between the latent and sensible heat fluxes, and a wrong simulation of their evolution can lead to errors in the temporal variations of the fluxes. However, these variables cannot be validated as they are not available on a continuous basis at most of FLUXNET sites (for this study we had soil water content data only for BVC, LW and ME). Finally, the various limitations of the eddy covariance method listed above can also alter the consistency of temporal variations in the measurements.

4.2. *Net carbon flux*

Figs. 5 and 6 also show the correlation coefficients between modelled and observed net ecosystem exchange (NEE). The variations of the net carbon flux are reproduced in a contrasting manner depending on the site. NEE correlations are generally lower than those of the energy fluxes. The annual cycle is poorly reproduced for SKo, SKy, CP, PO and BVS, due to a phase difference in the peak of carbon absorption in summer. The negative score for site ME is due to a shorter absorption period in the model than in the observations. As for LE and *H*, the summer diurnal variations seem better constrained than the seasonal ones, as shown by a narrower range of correlation values. Overall, the best scores are obtained for GU, HV, SO, WB, BX, LO, TH and SH, while the worst are found for ME, SKy, CP, PO, BVS, BVC and UP. Table 6 shows mean annual values and RMSEs for GPP reconstructed from observations and simulated by ISBA-CC. GPP is reconstructed by fitting nocturnal NEE and temperature with a Q_{10} function for 15 days periods, and by extrapolating diurnal values to calculate the ecosystem respiration Reco. Reconstructed GPP is then calculated as the difference between NEE and Reco. It must be noted that this method is equivalent to model Reco as a function of temperature only, without taking account other variables such as soil water content. There is a good agreement between modelled and reconstructed values for about half of sites. Differences are quite large for the second half of sites, again including the sites with poor scores for the other fluxes (e.g. SKy, CP, PO, BVS, BVC). These results show that the performances of the model to simulate the energy, the water and the carbon fluxes are closely related. The best results are obtained for deciduous broadleaf forests and coniferous forests, while the three agricultural sites are systematically among the sites having the lowest scores. However, this result must be regarded with caution, as only a few sites and years of data are available for evergreen broadleaf forests, crops and natural grasslands.

As for turbulent heat fluxes, differences between the model and the measurements can be attributed to uncertainties in the forcing climatic variables, in the model formulation and parameterization, and in the observed fluxes. The quality of the net carbon flux simulation depends on the realism of several variables in the model. In particular, the poor correlations at agricultural sites PO, BVS and BVC are probably explained by a wrong simulation of the vegetation growth cycle, as practices such as sowing or irrigation are not taken into account in the model. Moreover, the net ecosystem exchange is the balance between two large and opposite fluxes, the gross primary production and the ecosystem respiration. A small error in these fluxes produces a large one in the net flux, and can even lead to an error in the flux sign. Concerning the observations, it is likely that the flaws responsible for the non-closure of the energy balance also impact the quality of the net carbon flux measurements (Twine et al., 2000; Wilson et al., 2002). Also, the under-estimation of the night-time carbon flux by the eddy covariance method (Baldocchi et al., 2001) can produce an erroneous shape of the diurnal cycle. Likewise, lateral air advection has been pointed out recently as a large source of error in estimated fluxes (Papale et al., 2006; Sun et al., 2007).

Table 6 – Mean values (calculated with all dates for which measurements are available) and RMSE between monthly means of gross primary production (GPP) (g C m^{-2} day^{-1}) reconstructed from observations and simulated by the model at the 26 FLUXNET sites

Code	Reconstructed GPP	Modelled GPP	RMSE GPP
GU	2.9	2.4	1.2
HE	4.5	6.5	2.7
HV	3.4	3.0	2.2
SO	4.2	3.8	1.5
VI	4.4	4.5	1.8
WB	4.6	7.9	4.3
FL	1.8	2.3	1.8
HY	2.9	3.2	1.3
NO	7.0	3.4	4.6
AB	5.2	4.3	1.8
BR	2.9	5.2	3.3
BX	5.0	5.3	1.8
LO	4.1	4.8	1.9
ME	4.2	4.0	2.7
TH	5.2	4.6	1.6
WE	3.6	4.0	1.8
SKo	2.0	2.7	3.3
SKy	1.1	3.3	4.1
CP	5.1	8.5	5.3
PO	3.1	6.3	6.0
BVS	2.3	4.7	5.4
BVC	4.3	6.3	4.5
UP	0.9	0.9	0.3
LW	1.6	5.0	5.6
FI	–	–	–
SH	5.5	9.0	4.8

ISBA-CC includes a complex parameterization of heterotrophic respiration, which deals with the effect of soil moisture on the soil organic matter decomposition. To assess if this parameterization allows an improvement of the net carbon flux simulation, we investigated the link between the net carbon flux and the soil water content (SWC), both in the observations and in the two versions of the land surface model, ISBA-A-gs and ISBA-CC. We calculated the correlations between the daily means of these two variables, selecting only night-time measurements to eliminate the contribution of gross primary production from the net flux. Daily means are organized in temperature classes of 5 K range, in order to reduce the influence of the background correlations between respiration and soil moisture with temperature. As the soil water content is seldom measured at FLUXNET sites, we used the modelled SWC to calculate the correlations with observed NEE, after we verified that the correlations are similar to those obtained with observed SWC at sites where data are available

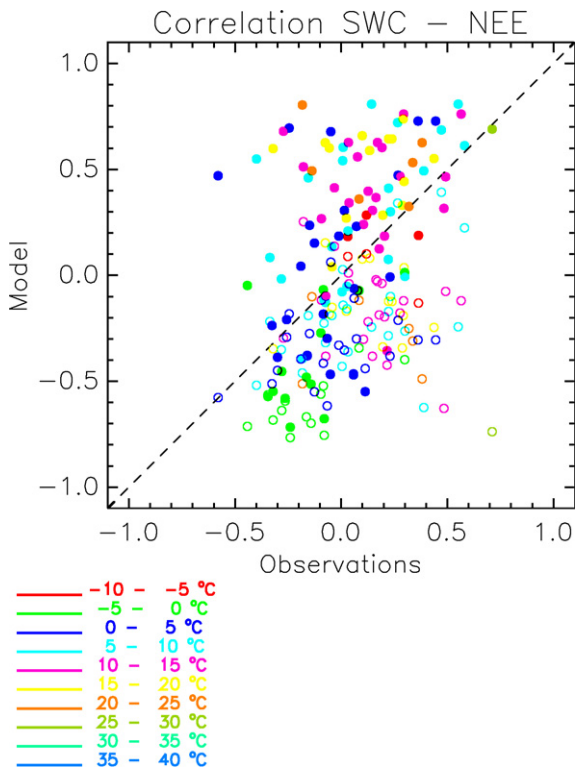

Fig. 7 – Scatter plot of correlations between the modelled SWC and the observed NEE (X axis) and between the modelled SWC and NEE (Y axis) simulated by ISBA-A-gs (open circles) and ISBA-CC (solid circles). Colours correspond to various ranges of temperature (see legend).

(ME, BVC and LW). Fig. 7 compares the correlations between SWC and observed NEE with those obtained with modelled NEE by ISBA-A-gs and ISBA-CC, respectively. Concerning the observations, most of sites show temperature ranges for which absolute correlations values are higher than 0.2, denoting a partly linear relationship between the two variables. Overall, observed correlations are positive for the highest temperatures, and negative for the lowest ones. As the ecosystem respiration only depends on soil temperature in ISBA-A-gs (Rivalland et al., 2005), this version of the model systematically produces negative correlations, due to the negative correlation between temperature and soil moisture. On the contrary, ISBA-CC is able to produce both negative correlations at high temperatures, and positive correlations at low temperatures, thanks to its parameterization of heterotrophic respiration and its response to soil moisture. At high temperatures (at the end of Spring, in Summer or at the beginning of Autumn), the soil water content is usually between the wilting point and the field capacity, and an increase in soil moisture enhances the microbial activity (see Eq. (B.8)). At low temperatures (at the end of Autumn, in Winter or at the beginning of Spring) the soil water content is often between field capacity and saturation, and an increase in soil moisture tends to reduce available oxygen and to limit decomposition. Therefore, the new version of the model improves the representation of the net carbon flux. This skill is of particular importance for studying the response of the terrestrial biosphere to future climate changes. Indeed, a strong decrease in net primary productivity has been observed during the heat wave of summer 2003 in Europe, due to a reduction of gross primary production but also of ecosystem respiration, contrary to what could be expected as a result of an increase in temperature (Ciais et al., 2005; Granier et al., 2007; Reichstein et al., 2007). These anomalies were mainly driven by limitation of water rather than by higher temperatures. Such extreme climate events are likely to be more frequent in the next decades over numerous regions of the globe due to the anthropogenic climate change (Meehl et al., 2007).

Finally, Table 7 compares the carbon pools in vegetation and in soil collected by Houghton (1999) and simulated by ISBA-CC, grouped by ecosystems. The model overestimates biomass for the three ecosystems of forest. This result can be explained by the parameters values, in particular by the vegetation fraction, which is quite high for forests (see Section 4.1). Carbon in vegetation is underestimated for grasslands, but this result (and the associated high value of standard deviation) is mainly due to the tundra UP site, encountering unfavourable conditions for photosynthesis. Moreover, biomass of herbaceous vegetation types has a strong annual cycle, and the maximum values are about twice the mean values of Table 7 for grasslands and crops. The size of soil pools is much larger in the model than in Houghton (1999). However, the mean values in Houghton (1999) are obtained from measurements in the first meter of soil, while the model values are calculated as the sum of the carbon in all litter and soil reservoirs. As the model does not simulate the vertical distribution of carbon, a direct comparison is not possible. It

Table 7 – Statistics about carbon stocks in vegetation and soil for various ecosystems: mean values collected by Houghton (1999) and simulated by ISBA-CC (Mg C ha^{-1}), standard deviation for ISBA-CC, number of FLUXNET sites

Ecosystem	C vegetation (Houghton, 1999)	C vegetation ISBA-CC	STD C vegetation ISBA-CC	C soil (Houghton, 1999)	C soil ISBA-CC	STD C soil ISBA-CC	N
Boreal forests	90	127	49	200	295	99	4
Evergreen temperate forests	160	170	40	130	319	80	10
Deciduous temperate forests	135	191	52	130	297	76	5
Grasslands	7	4	3	190	312	139	4
Crops	5	5	1	–	460	129	3

For ISBA-CC, stocks in vegetation and soil are obtained by adding the reservoirs listed in Tables 2 and 3, respectively.

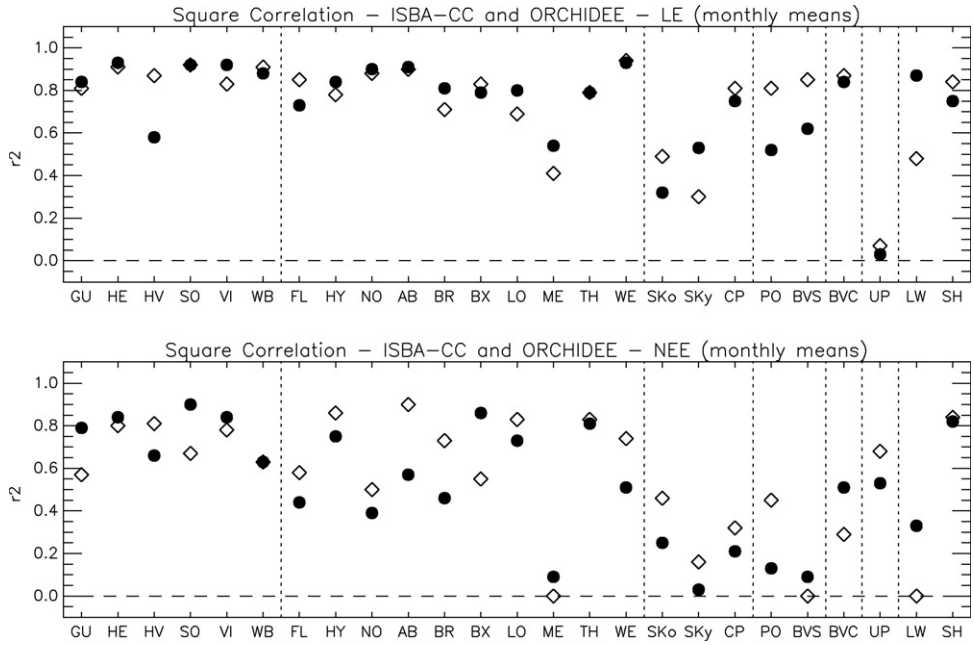

Fig. 8 – Square correlations between the monthly means of the fluxes measured at FLUXNET sites and simulated by ISBA-CC (solid circles) and by ORCHIDEE (open diamonds) for LE (a) and NEE (b). Vegetation types are divided by vertical lines, from left to right: DBF, NLF, EBF, CC3, CC4, HC3, HC4.

must also be noted that these values of soil carbon are those simulated at equilibrium. The values of soil carbon for cultivated areas are highly variable in Houghton (1999) (from 32 to 165 MgC ha^{-1}) and no mean value has been indicated in Table 7. Anyway, the simulated values cannot be directly compared to those of Houghton (1999) for crops, as the model does not simulate agricultural practices such as harvesting and ploughing. Overall, Table 7 shows that the model simulates realistic values of carbon in biomass and soil.

4.3. *Comparison with ORCHIDEE*

Krinner et al. (2005) have run the ORCHIDEE model on the same FLUXNET sites used in this study and have calculated statistics between their simulations and the measurements (ftp://ftp.agu.org/apend/gb/2003GB002199). This offers the opportunity to compare ISBA-CC with a state-of-the-art terrestrial carbon model. Figs. 8 and 9 show the square correlations between in-situ measurements and the two

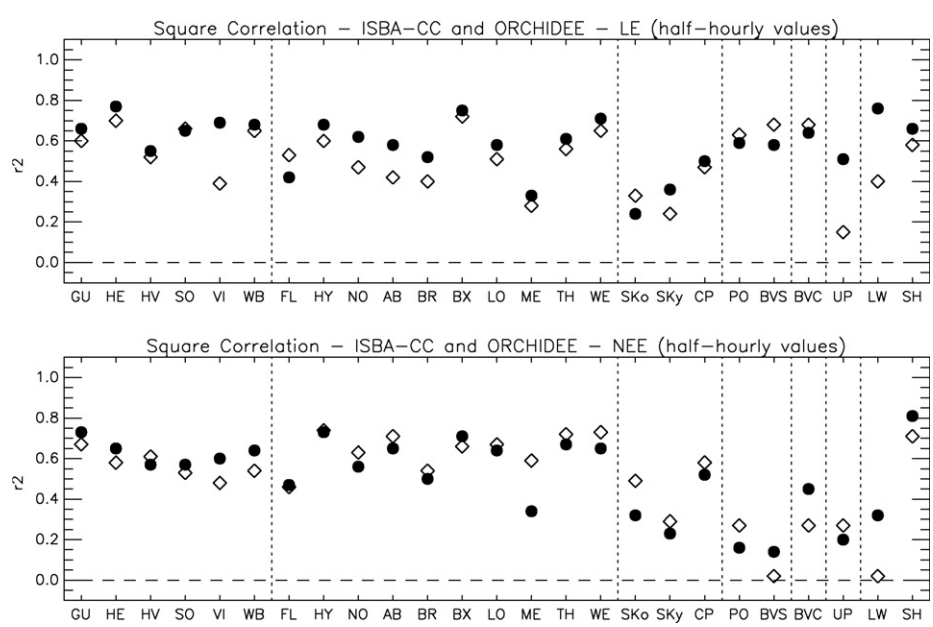

Fig. 9 – Same as Fig. 8 but for half-hourly values.

models for LE and NEE at seasonal and diurnal timescales. The correlations obtained by ISBA-CC and ORCHIDEE are very close for most of sites for the latent heat flux. No model systematically proved better than the other. At some sites, ORCHIDEE performs better than ISBA-CC (e.g. at FL, SKo, PO, BVS), but the opposite is also obtained for about the same number of sites (VI, BR, SKy, LW). The seasonal differences between the two models are more pronounced for the net carbon flux. ORCHIDEE (ISBA-CC) variations are closer to observations for 13 (8) sites. As we noticed before, correlations are generally lower for NEE than for LE, and the lowest scores are obtained at the same sites for the two models (ME, SKy, CP and BVS). This latter result suggests that the differences between the simulations and the observations come from atmospheric forcing or flux measurements uncertainties (see Section 4.1), or from the same shortcomings in the two models. ORCHIDEE and ISBA-CC share the same parameterization of heterotrophic respiration, but it is unlikely that this parameterization is responsible for the common lowest scores for NEE at these sites, as the two models also jointly obtain poor scores for the energy fluxes, notably for net radiation. The other processes (energy budget, hydrology, photosynthesis) are treated differently, but the two models are based on the same general assumptions: for example both of them are big-leaf models, resolving a single energy budget for soil and vegetation within a tile; also, the versions used in this study represent crops as perennial grasslands, without taking agricultural practices into account (for PO, BVS and BVC); moreover, Mediterranean sites (CP, SKo and SKy) are treated as evergreen broadleaf forests by both ORCHIDEE and ISBA-CC, while this type is dedicated to represent evergreen tropical forests.

ISBA-CC also favourably compares with other models validated with the FLUXNET data set in other studies. For example, the bias between the observed and simulated energy fluxes are of the same magnitude than those found by Stöckli and Vidale (2005) at forest sites CP, VI, TH, GU and NO. Also, Morales et al. (2005) inter-compared four terrestrial ecosystem models (GOTILWA+, LPJ-GUESS, ORCHIDEE and RHESSys) at 15 forest sites of the EUROFLUX network, 11 of which are used in this study. ISBA-CC often gets the best statistics for LE and thus confirms the skill of ISBA for reproducing hydrological processes already emphasized in several inter-comparison projects (e.g. Boone et al., 2004; Decharme and Douville, 2007). Results are more different for NEE, but overall, ISBA-CC obtains similar scores than those of the other models.

5. Summary and conclusion

This study presents a new version of the ISBA land surface model, ISBA-CC, which simulates the main processes of the terrestrial carbon cycle, i.e. the evolution of the carbon reservoirs in the vegetation and in the soil, and the net ecosystem exchange flux components (gross primary production, autotrophic and heterotrophic respiration). The simulated energy and carbon fluxes are validated against in-situ measurements at 26 FLUXNET sites located at temperate and high latitudes of the Northern Hemisphere, sampling the main biomes present in the area.

- Overall, the model represents well the temporal variations in the fluxes, both at diurnal, seasonal and inter-annual scales. Nevertheless, the model obtains poor scores for some sites. Our study shows that there is a close relationship between the scores obtained by the model for the various fluxes. For example, defaults in the simulation of net radiation have repercussions on the latent heat, the sensible heat and the net carbon fluxes at ME and SKy sites. This result emphasizes the interest of the validation against the FLUXNET dataset, which provides coherent measurements of all these fluxes.
- The best results are generally obtained for deciduous broadleaf forests and coniferous forests. Results are more variable for the other vegetation types, but no definitive conclusion can be drawn about the performances of the model for representing the various vegetation types, as fewer sites and years of data are available for evergreen broadleaf forests, grasslands and crops. In the future, the model will also be validated over tropical ecosystems.
- Correlation coefficients with observations are generally lower for the net ecosystem exchange flux than for the energy fluxes, showing that the parameterization of the carbon processes is less robust than the parameterization of the energy processes at this time in the model. However, ISBA-CC obtains similar scores than those of other state-of-the-art terrestrial ecosystem models.
- The parameterization of heterotrophic respiration used in ISBA-CC takes into account the effect of soil water content on the variations of the carbon emissions. This formulation allows a better simulation of the observed link between the carbon flux and the soil water content compared to ISBA-A-gs. This skill is of particular importance for regions experiencing strong variations in precipitation and in soil water availability.
- The comparison with observations suggests several improvements in the model, namely the representation of the fraction of vegetation and the simulation of agricultural practices, such as sowing or irrigation. Apart from the model formulation and parameterization, the differences between the simulations and the measurements also can be attributed to the errors in the atmospheric forcing gap-filling, and to uncertainties in the flux measurements due to the eddy covariance method. In this respect, it would be helpful to systematically measure and make available other surface variables together with the fluxes at FLUXNET sites, such as LAI and soil water content, to clearly establish the causes of the discrepancies between the models and the observations.
- Finally, this study shows encouraging results for using ISBA-CC to assess the response of the terrestrial biosphere to future climate changes, as the model matches the observed flux variability driven by climate. When coupled with a general circulation model, this new land surface model will also allow an analysis of the retroactions between the climate and the carbon cycle.

Acknowledgements

The authors thank all the investigators of CarboEurope, AmeriFlux and FIFE sites used in this study for collecting

the data. We also thank the people involved in the FLUXNET data archive, for creating an essential tool for validation and improvement of terrestrial models at a local and a global scale. We are also grateful to two anonymous reviewers for their constructive remarks, which helped to improve the quality of this manuscript.

Appendix A. The growth model

A.1. Respiration

The leaf respiration is the same as in Calvet et al. (1998). The model first calculates the photosynthesis rate in light-saturating conditions A_m (mg CO_2 m^{-2} s^{-1}) and then calculates the dark respiration R_d (mg CO_2 m^{-2} s^{-1}) as:

$$R_d = \frac{A_m}{9} \tag{A.1}$$

The dark respiration flux is integrated over the canopy:

$$R_{dC} = \mathrm{LAI}\, R_d \tag{A.2}$$

Finally R_{dC} is averaged over 1 day and converted into kg m^{-2} day^{-1} to obtain the daily flux R_{BL}:

$$R_{B_L} = \sum_{1\,\mathrm{day}} 10^{-6} \frac{M_C}{P_C\, M_{CO_2}} R_{dC}\, dt \tag{A.3}$$

where dt is the model time step (s), P_C is the proportion of carbon in the dry plant biomass (40%), and M_C and M_{CO_2} are the molecular weights of carbon and CO_2 (12 and 44 g mol^{-1}, respectively).

The respiration of $B_{s,act}$ (kg m^{-2} day^{-1}) is calculated following Calvet and Soussana (2001):

$$R_{B_{s,act}} = \eta_R\, Q_{10}^{(T_s-25)/10}\, B_{s,act} \tag{A.4}$$

where T_s is the surface temperature (in °C), η_R is a respiration coefficient of 1% of $B_{s,act}$ per day, and $Q_{10} = 2$.

The other structural reservoirs respiration is calculated according to the linear formulation proposed by Ruimy et al. (1996):

$$R_{B_{s,pas}} = R_0(1 + 0.16\, T_s) B_{s,pas} \tag{A.5}$$

$$R_{B_{s,bg}} = R_0(1 + 0.16\, T_p) B_{s,bg} \tag{A.6}$$

where T_p is the soil temperature (in °C), R_0 is the value of respiration at 0 °C, taken to 1.19 g g^{-1} day^{-1} (the value for sapwood reservoir in Ruimy et al., 1996).

$B_{w,ag}$ and $B_{w,bg}$ are wood reservoirs and do not respire.

A.2. Decline

The other term of decrease in biomass is called decline. It includes decreases due to mortality and reallocation to other reservoirs. The decline term D_B of the biomass B is calculated by the generic equation:

$$D_B = B(1 - e^{-\Delta t/\tau_B}) \tag{A.7}$$

where $\Delta t = 1$ day and τ_B is a residence time (in days) which depends on the reservoir B.

τ_{BL} varies in time and is calculated as in ISBA-A-gs (Calvet et al., 1998). It depends on the maximum span time of the leaf biomass, τ_M, on the maximum leaf net assimilation reached on the day before time t, $A_{nfm}(t)$, calculated by the model, and on the optimum leaf net assimilation, $A_{n,\,max}$.

$$\tau_{BL}(t) = \tau_M \frac{A_{nfm}(t)}{A_{n,\,max}} \tag{A.8}$$

The other residence times are constant. In order to limit the number of parameters in the model, the residence times of structural biomass reservoirs are defined as a function of τ_M.

$$\tau_{Bs,\,act} = \tau_M \tag{A.9}$$

$$\tau_{Bs,\,pas} = \frac{\tau_M}{4} \tag{A.10}$$

$$\tau_{Bs,\,bg} = \tau_M \tag{A.11}$$

The same parameter τ_w is used for above and below ground woody biomass reservoirs and depends on the vegetation type. Values of τ_M and τ_w are listed in Table 4.

A.3. Storage, allocation and mortality

A part of the decline term D_B represents mortality (M_B), and will feed the litter pools of the heterotrophic respiration parameterization. The remaining part of decline is a storage term (S_B), which is allocated to other biomass reservoirs. As in Calvet and Soussana (2001), the division of the decline term between storage and mortality depends on the evolution of the leaf biomass B_L. Leaf biomass increases with the net assimilation of carbon by photosynthesis (difference between the gross photosynthesis and the leaf respiration), and decreases according to the decline term D_{BL}. In the growing phase, i.e. when the net balance between these two contributions is positive, all decline is converted to storage, whereas in case of leaf senescence (negative balance), only a half of the decline term is assigned to storage. Storage of $B_{s,bg}$ is equal to zero in the case of herbaceous species. Storage is equal to zero for woody biomass reservoirs anyway.

Allocation of carbon to B_L, $B_{s,act}$ and $B_{s,pas}$ is the same as in Calvet and Soussana (2001). B_L is supplied by gross assimilation, and the evolution of B_L, $B_{s,act}$ and $B_{s,pas}$ are linked by the nitrogen dilution relationship during the growing phase. During senescence, $B_{s,act}$ and $B_{s,pas}$ do not receive input biomass.

The allocation to the structural below ground reservoir is given by:

$$A_{Bs,bg} = f_{S,BL,Bs,bg} S_{BL} + f_{S,Bs,act,Bs,bg} S_{Bs,act} + f_{S,Bs,pas,Bs,bg} S_{Bs,pas} \quad (A.12)$$

where $f_{S,BL,Bs,bg}$, $f_{S,Bs,act,Bs,bg}$, and $f_{S,Bs,pas,Bs,bg}$ are the fraction of S_{BL}, $S_{Bs,act}$ and $S_{Bs,pas}$ allocated to $B_{s,bg}$, respectively. During the growing phase, $f_{S,BL,Bs,bg}$ is time varying and is the remaining fraction of S_{BL} after allocation to $B_{s,act}$ according to the nitrogen dilution relationship. During leaf senescence, $f_{S,BL,Bs,bg} = 1$. $f_{S,Bs,act,Bs,bg}$ and $f_{S,Bs,pas,Bs,bg}$ are constant. They are fixed to 1 for herbaceous plants and 0.3 for woody plants during the growing phase and are set to 0 during senescence. These fraction values were chosen to obtain both realistic shoot to root biomass ratio and accumulation of woody biomass in the case of forest vegetation types.

Woody reservoirs are supplied only for woody vegetation types:

$$A_{Bw,ag} = (1 - f_{S,Bs,act,Bs,bg}) S_{Bs,act} + (1 - f_{S,Bs,pas,Bs,bg}) S_{Bs,pas} \quad (A.13)$$

$$A_{Bw,bg} = S_{Bs,bg} \quad (A.14)$$

Finally, mortality is diagnosed as the difference between decline and storage by the following generic equation for each reservoir B:

$$M_B = D_B - S_B \quad (A.15)$$

Appendix B. The heterotrophic respiration parameterization

B.1. Distribution of dead organic matter in the litter pools

The mortality fluxes M_B calculated by the growth model are distributed in the litter pools according to the position of the biomass reservoirs above or below the surface and the lignin content of the residues. $f_{M,m}$, the fraction of M_B going into metabolic litter is given by (Parton et al., 1987):

$$f_{M,m} = 0.85 - 0.018 \frac{L_B}{N_B} \quad (B.1)$$

Table B1 – Values of the lignin to nitrogen ratio of the biomass reservoirs

Biomass reservoir	L_B/N_B
B_L	8.8
$B_{s,act}$	14
$B_{s,pas}$	14
$B_{s,bg}$	14
$B_{w,ag}$	14
$B_{w,bg}$	14

Table B2 – Values of the maximum decomposition rate parameter (day^{-1})

Carbon pool	K_C
$LC_{s,ag}$	1.12×10^{-2}
$LC_{m,ag}$	4.15×10^{-2}
$LC_{s,bg}$	1.12×10^{-2}
$LC_{m,bg}$	4.15×10^{-2}
SC_{act}	1.84×10^{-2}
SC_{slow}	5.10×10^{-4}
SC_{pas}	1.13×10^{-5}

where L_B/N_B is the lignin to nitrogen ratio in the biomass reservoir B. Values of L_B/N_B are given in Table B1 for each reservoir.

The remaining fraction, $f_{M,s}$, is allocated to structural litter:

$$f_{M,s} = 1 - f_{M,m} \quad (B.2)$$

B.2. Decomposition of organic matter in the soil

The evolution of the soil carbon state variables is calculated following Parton et al. (1987):

$$\frac{dC}{dt} = K_C^a c_T(T) c_w(w) C \quad (B.3)$$

where C (g C m^{-2}) is one of the carbon pool of Table 3, K_C^a (day^{-1}) is the maximum decomposition rate of the carbon pool C, c_T and c_w are normalized functions dealing with the effect on decomposition of soil temperature and moisture, respectively.

The maximum decomposition rates K_C^a are constant and equal to values of K_C listed in Table B2 for all carbon pools, except for $LC_{s,ag}$ and $LC_{s,bg}$, which are a function of the lignin content of the structural material, and for SC_{act}, which is a function of the soil texture (Parton et al., 1987).

$$K^a_{LCs,ag} = K_{LCs,ag} e^{-3 Ls,ag} \quad (B.4)$$

$$K^a_{LCs,bg} = K_{LCs,bg} e^{-3 Ls,bg} \quad (B.5)$$

$$K^a_{SCact} = K_{SCact}(1 - 0.75 (f_{silt} + f_{clay})) \quad (B.6)$$

where $L_{s,ag}$ and $L_{s,bg}$ are the lignin fraction in $LC_{s,ag}$ and $LS_{s,bg}$, respectively, and f_{silt} and f_{clay} are the silt and clay fractions in the soil.

As the soil organic matter model is used in the framework of a land surface model, c_T and c_w are expressed as functions of instantaneous soil temperature and moisture calculated by the model, following Krinner et al. (2005). Moreover, c_w is modified to take into account the limiting effect of high values of soil moisture on decomposition.

$$c_T(T) = 2^{(T-30)/10} \quad (B.7)$$

$$c_w(w) = \min(0.05, \max(1, a\,\theta^2_{\mathrm{wilt,fc}} + b\,\theta_{\mathrm{wilt,fc}} + c)), \text{ if } w \le w_{\mathrm{fc}}$$
$$c_w(w) = \max(0.5, 1 - 0.5\,\theta_{\mathrm{fc,sat}}), \quad \text{if } w > w_{\mathrm{fc}} \tag{B.8}$$

with $a = -1.1$, $b = 2.4$, $c = -0.29$, and:

$$\theta_{\mathrm{wilt,fc}} = \frac{w - w_{\mathrm{wilt}}}{w_{\mathrm{fc}} - w_{\mathrm{wilt}}}$$
$$\theta_{\mathrm{fc,sat}} = \frac{w - w_{\mathrm{fc}}}{w_{\mathrm{sat}} - w_{\mathrm{fc}}} \tag{B.9}$$

where T is the soil temperature in °C, w is the soil water content in $m^3\ m^{-3}$, w_{wilt}, w_{fc} and w_{sat} are the soil water content at wilting point, field capacity and saturation, respectively. For the above ground litter pools, the temperature and soil moisture variables in Eqs. (B.3), (B.7)–(B.9) are the surface variables of the ISBA model, while for the below ground litter pools and soil carbon pools, they are the variables representative of the deep soil layer.

B.3. Carbon fluxes

The decomposition of organic matter dC/dt in soil carbon pool C (Eq. (B.3)) consists of several carbon fluxes (Parton et al., 1987). A part of carbon is mineralized and rejected as CO_2 into the atmosphere, while the remaining part is redistributed towards the other soil reservoirs. The fractions $f_{C,C'}$ multiplying dC/dt to form each flux from pool C to pool C' follow Parton et al. (1987) and are detailed below (the sum of all fractions is 1 for each pool C):

$$f_{\mathrm{LC_{s,ag}, SC_{act}}} = 0.55\,(1 - L_{\mathrm{s,ag}})$$
$$f_{\mathrm{LC_{s,ag}, SC_{slow}}} = 0.7\,L_{\mathrm{s,ag}}$$
$$f_{\mathrm{LC_{s,ag}, CO_2}} = 0.45 - 0.15\,L_{\mathrm{s,ag}} \tag{B.10}$$

$$f_{\mathrm{LC_{m,ag}, SC_{act}}} = 0.45$$
$$f_{\mathrm{LC_{m,ag}, CO_2}} = 0.55 \tag{B.11}$$

$$f_{\mathrm{LC_{s,bg}, SC_{act}}} = 0.45\,(1 - L_{\mathrm{s,bg}})$$
$$f_{\mathrm{LC_{s,bg}, SC_{slow}}} = 0.7\,L_{\mathrm{s,bg}}$$
$$f_{\mathrm{LC_{s,bg}, CO_2}} = 0.55 - 0.25\,L_{\mathrm{s,bg}} \tag{B.12}$$

$$f_{\mathrm{LC_{m,bg}, SC_{act}}} = 0.45$$
$$f_{\mathrm{LC_{m,bg}, CO_2}} = 0.55 \tag{B.13}$$

$$f_{\mathrm{SC_{act}, SC_{slow}}} = 0.146 + 0.68\,(f_{\mathrm{silt}} + f_{\mathrm{clay}})$$
$$f_{\mathrm{SC_{act}, SC_{pas}}} = 0.004$$
$$f_{\mathrm{SC_{act}, CO_2}} = 0.85 - 0.68\,(f_{\mathrm{silt}} + f_{\mathrm{clay}}) \tag{B.14}$$

$$f_{\mathrm{SC_{slow}, SC_{act}}} = 0.42$$
$$f_{\mathrm{SC_{slow}, SC_{pas}}} = 0.03$$
$$f_{\mathrm{SC_{slow}, CO_2}} = 0.55 \tag{B.15}$$

$$f_{\mathrm{SC_{pas}, SC_{act}}} = 0.45$$
$$f_{\mathrm{SC_{pas}, CO_2}} = 0.55 \tag{B.16}$$

REFERENCES

Arora, V.K., 2002. Modeling vegetation as a dynamic component in soil-vegetation-atmosphere transfer schemes and hydrological models. Rev. Geophys. 40 (2).

Baldocchi, D., Falge, E., Gu, L., Olson, R., Hollinger, D., Running, S., Anthoni, P., Bernhofer, C., Davis, K., Evans, R., Fuentes, J., Goldstein, A., Katul, G., Law, B., Lee, X., Malhi, Y., Meyers, T., Munger, W., Oechel, W., Paw, K.T., Pilegaard, K., Schmid, H.P., Valentini, R., Verma, S., Vesala, T., Wilson, K., Wofsy, S., 2001. FLUXNET: a new tool to study the temporal and spatial variability of ecosystem-scale carbon dioxide, water vapor, and energy flux densities. Bull. Am. Meteor. Soc. 82, 2415–2434.

Berbigier, P., Bonnefond, J.-M., Mellman, P., 2001. CO_2 and water vapour fluxes for two years above Euroflux forest site. Agric. For. Meteorol. 108, 183–197.

Betts, A.K., Ball, J.H., 1998. FIFE surface climate and site-average dataset 1987–89. J. Atmos. Sci. 55, 1091–1108.

Boone, A., Habets, F., Noilhan, J., Clark, D., Dirmeyer, P., Fox, S., Gusev, Y., Haddeland, I., Koster, R., Lohmann, D., Mahanama, S., Mitchell, K., Nasonova, O., Niu, G.-Y., Pitman, A., Polcher, J., Shmakin, A.B., Tanaka, K., van den Hurk, B., Vérant, S., Verseghy, D., Viterbo, P., Yang, Z.-L., 2004. The Rhône-aggregation land surface scheme intercomparison project: an overview. J. Climate 17, 187–208.

Calvet, J.-C., 2000. Investigating soil and atmospheric plant water stress using physiological and micrometeorological data. Agric. For. Meteorol. 103, 229–247.

Calvet, J.-C., Soussana, J.-F., 2001. Modelling CO_2-enrichment effects using an interactive vegetation SVAT scheme. Agric. For. Meteorol. 108, 129–152.

Calvet, J.-C., Noilhan, J., Roujean, J.-L., Bessemoulin, P., Cabelguenne, M., Olioso, A., Wigneron, J.-P., 1998. An interactive vegetation SVAT model tested against data from six contrasting sites. Agric. For. Meteorol. 92, 73–95.

Calvet, J.-C., Rivalland, V., Picon-Cochard, C., Guehl, J.-M., 2004. Modelling forest transpiration and CO_2 fluxes—response to soil moisture stress. Agric. For. Meteorol. 124, 143–156.

Calvet, J.-C., Gibelin, A.-L., Roujean, J.-L., Martin, E., Le Moigne, P., Douville, H., Noilhan, J., 2007. Past and future scenarios of the effect of carbon dioxide on plant growth and transpiration for three vegetation types of south-western France. Atmos. Chem. Phys. Discuss. 7, 4761–4779.

Carrara, A., Kowalski, A., Neirynck, J., Janssens, I., Yuste, J.C., Ceulemans, R., 2003. Net ecosystem CO_2 exchange of mixed forest in Belgium over 5 years. Agric. For. Meteorol. 119, 209–227.

Ciais, P., Tans, P.P., White, J.W.C., Trolier, M., Francey, R.J., Berry, J.A., Randall, D.R., Sellers, P.J., Collatz, G., Schimel, D.S., 1995. Partitioning of ocean and land uptake of CO_2 as inferred by $\delta^{13}C$ measurements from the NOAA Climate Monitoring and Diagnostics Laboratory Global Air Sampling Network. J. Geophys. Res. 100, 5051–5070.

Ciais, P., Reichstein, M., Viovy, N., Granier, A., Ogée, J., Allard, V., Aubinet, M., Buchmann, N., Bernhofer, C., Carrara, A., Chevallier, F., De Noblet, N., Friend, A.D., Friedlingstein, P., Grünwald, T., Heinesch, B., Keronen, P., Knohl, A., Krinner, G., Loustau, D., Manca, G., Matteucci, G., Miglietta, F., Ourcival, J.M., Papale, D., Pilegaard, K., Rambal, S., Seufert, G., Soussana, J.F., Sanz, M.J., Schulze, E.D., Vesala, T., Valentini, R., 2005. Europe-wide reduction in primary productivity caused by the heat and drought in 2003. Nature 437, 529–533.

Collatz, G.J., Ribas-Carbo, M., Berry, J.A., 1992. Coupled photosynthesis-stomatal conductance model for leaves of C_4 plants. Aust. J. Plant Physiol. 19, 519–538.

Cox, P.M., Huntingford, C., Harding, R.J., 1998. A canopy conductance and photosynthesis model for use in a GCM land surface scheme. J. Hydrol. 212–213, 79–94.

Cox, P.M., Betts, R.A., Jones, C.D., Spall, S.A., Totterdell, I.J., 2000. Acceleration of global warming due to carbon-cycle feedbacks in a coupled climate model. Nature 408, 184–187.

Decharme, B., Douville, H., 2007. Global validation of the ISBA sub-grid hydrology. Climate Dyn. 29, 21–37.

Denman, K.L., Brasseur, G., Chidthaisong, A., Ciais, P., Cox, P.M., Dickinson, R.E., Hauglustaine, D., Heinze, C., Holland, E., Jacob, D., Lohman, U., Ramachandran, S., da Silva Dias, P.L., Wofsy, S.C., Zhang, X., 2007. Couplings between changes in the climate system and biogeochemistry. In: Solomon, S., Qin, D., Manning, M., Chen, Z., Marquis, M., Averyt, K.B., Tignor, M., Miller, H.L. (Eds.), Climate Change 2007: The Physical Science Basis. Contribution of Working Group I to the Fourth Assessment Report of the Intergovernmental Panel on Climate Change. Cambridge University Press, Cambridge, United Kingdom and New York, NY, USA.

Dickinson, R.E., Shaikh, M., Bryant, R., Graumlich, L., 1998. Interactive canopies for a climate model. J. Climate 11, 2823–2836.

Dolman, A.J., Moors, E.J., Elbers, J.A., 2002. The carbon uptake of a mid latitude pine forest growing on sandy soil. Agric. For. Meteorol. 111, 157–170.

Dufresne, J.-L., Berthelot, M., Bopp, L., Ciais, P., Fairhead, L., Le Treut, H., Monfray, P., 2002. On the magnitude of positive feedback between future climate change and the carbon cycle. Geophys. Res. Lett. 29.

Falge, E., Aubinet, M., Bakwin, P., Berbigier, P., Bernhofer, C., Black, A., Ceulemans, R., Dolman, A., Goldstein, A., Goulden, M., Granier, A., Hollinger, D., Jarvis, P., Jensen, N., Pilegaard, K., Katul, G., Kyaw Tha Paw, P., Law, B., Lindroth, A., Loustau, D., Mahli, Y., Manson, R., Moncrieff, P., Moors, E., Munger, W., Meyers, T., Oechel, W., Schulze, E., Thorgeirsson, H., Tenhunen, J., Valentini, R., Verma, S., Vesala, T., Wofsy, S., 2005. FLUXNET Marconi Conference Gap-Filled Flux and Meteorology Data, 1992–2000. Data set. Available on-line [http://www.daac.ornl.gov] from Oak Ridge National Laboratory Distributed Active Archive Center, Oak Ridge, Tennessee, U.S.A., doi:10.3334/ORNLDAAC/811.

Farquhar, G.D., von Caemmerer, S., Berry, J.A., 1980. A biochemical model of photosynthetic CO_2 assimilation in leaves of C_3 species. Planta 149, 78–90.

Foley, J.A., Prentice, I.C., Ramunkutty, N., Levis, S., Pollard, D., Sitch, S., Haxeltine, A., 1996. An integrated biosphere model of land surface processes, terrestrial carbon balance, and vegetation dynamics. Global Biogeochem. Cycles 10, 603–628.

Friedlingstein, P., Cox, P., Betts, R., Bopp, L., von Bloh, W., Brovkin, V., Cadule, P., Doney, S., Eby, M., Fung, I., Bala, G., John, J., Jones, C., Joos, F., Kato, T., Kawamiya, M., Knorr, W., Lindsay, K., Matthews, H.D., Raddatz, T., Rayner, P., Reick, C., Roeckner, E., Schnitzler, K.-G., Schnur, R., Strassmann, K., Weaver, A.J., Yoshikawa, C., Zeng, N., 2006. Climate-carbon cycle feedback analysis: results from the C^4MIP Model intercomparison. J. Climate 19, 3337–3353.

Gibelin, A.-L., Calvet, J.-C., Roujean, J.-L., Jarlan, L., Los, S.O., 2006. Ability of the land surface model ISBA-A-gs to simulate Leaf Area Index at the global scale: comparison with satellites products. J. Geophys. Res. 111, D18102.

Goudriaan, J., van Laar, H.H., van Keulen, H., Louwerse, W., 1985. Photosynthesis, CO_2, and plant production. In: Day, W., Atkin, R.K. (Eds.), Weat Growth and Modelling. Vol. 86 of NATA ASI Series, Series A. Plenum Press, New York, pp. 107–122.

Goulden, M.L., Munger, J.W., Fan, S.-M., Daube, B.C., Wofsy, S.C., 1996. Exchange of carbon dioxide by a deciduous forest: response to interannual climate variability. Science 271, 1576–1578.

Granier, A., Ceschia, E., Damesin, C., Dufrene, E., Epron, D., Gross, P., Lebaube, S., Dantec, V.L., Goff, N.L., Lemoine, D., Lucot, E., Ottorini, J.M., Pontailler, J.Y., Saugier, B., 2000. The carbon balance of a young beech forest. Funct. Ecol. 14, 312–325.

Granier, A., Reichstein, M., Bréda, N., Janssens, I.A., Falge, E., Ciais, P., Grünwald, T., Aubinet, M., Berbigier, P., Bernhofer, C., Buchmann, N., Facini, O., Grassi, G., Heinesch, B., Ilvesniemi, H., Keronen, P., Knohl, A., Köstner, B., Lagergren, F., Lindroth, A., Longdoz, B., Lousteau, D., Mateus, J., Montagnani, L., Nys, C., Moors, E., Papale, D., Peiffer, M., Pilegaard, K., Pita, G., Pumpanen, J., Rambal, S., Rebmann, C., Rodrigues, A., Seufert, G., Tenhunen, J., Vesala, T., Wang, Q., 2007. Evidence for soil water control on carbon and water dynamics in European forests during the extremely dry year: 2003. Agric. For. Meteorol. 143, 123–145.

Houghton, R.A., 1999. The annual net flux of carbon to the atmosphere from changes in land use 1850–1990. Tellus 51B, 298–313.

Jacobs, C.M.J., van den Hurk, B.J.J.M., de Bruin, H.A.R., 1996. Stomatal behaviour and photosynthetic rate of unstressed grapevines in semi-arid conditions. Agric. For. Meteorol. 80, 111–134.

Krinner, G., Viovy, N., de Noblet-Ducoudré, N., Ogée, J., Polcher, J., Friedlingstein, P., Ciais, P., Sitch, S., Prentice, I., 2005. A dynamic global vegetation model for studies of the coupled atmosphere-biosphere system. Global Biogeochem. Cycles 19.

Law, B.E., Thornton, P.E., Irvine, J., Anthoni, P.M., Van Tuyl, S., 2001. Carbon storage and fluxes in ponderosa pine forests at different developmental stages. Global Change Biol. 7, 755–777.

Law, B.E., Falge, E., Gu, L., Baldocchi, D.D., Bakwin, P., Berbigier, P., Davis, K., Dolman, A.J., Falk, M., Fuentes, J.D., Goldstein, A., Granier, A., Grelle, A., Hollinger, D., Janssens, I.A., Jarvis, P., Jensen, N.O., Katul, G., Mahli, Y., Matteucci, G., Meyers, T., Monson, R., Munger, W., Oechel, W., Olson, R., Pilegaard, K., Paw, U.K.T., Thorgeirsson, H., Valentini, R., Verma, S., Vesala, T., Wilson, K., Wofsy, S., 2002. Environmental controls over carbon dioxide and water vapor exchange of terrestrial vegetation. Agric. For. Meteorol. 113, 97–120.

Lindroth, A., Grelle, A., Moren, A.S., 1998. Long-term measurements of boreal forest carbon balance reveal large temperature sensitivity. Global Change Biol. 4, 443–450.

Masson, V., Champeaux, J.-L., Chauvin, F., Meriguet, C., Lacaze, R., 2003. A global database of land surface parameters at 1-km resolution in meteorological and climate models. J. Climate 16, 1261–1282.

Meehl, G.A., Stocker, T.F., Collins, W.D., Friedlingstein, P., Gaye, A.T., Gregory, J.M., Kitoh, A., Knutti, R., Murphy, J.M., Noda, A., Raper, S.C.B., Watterson, I.G., Weaver, A., Zhao, Z.-C., 2007. Global climate projections. In: Solomon, S., Qin, D., Manning, M., Chen, Z., Marquis, M., Averyt, K.B., Tignor, M., Miller, H.L. (Eds.), Climate Change 2007: The Physical Science Basis. Contribution of Working Group I to the Fourth Assessment Report of the Intergovernmental Panel on Climate Change.. Cambridge University Press, Cambridge, United Kingdom and New York, NY, USA.

Meyers, T.P., 2001. A comparison of summertime water and CO_2 fluxes over rangeland for well watered and drought conditions. Agric. For. Meteorol. 106, 205–214.

Morales, P., Sykes, M.T., Prentice, I.C., Smith, P., nd, H., Bugmann, B.S., Zierl, B., Friedlingstein, P., Viovy, N., Sabaté, S., Sanchez, A., Pla, E., Garcia, C.A., Sitch, S., Arneth, A., Ogée, J., 2005. Comparing and evaluating process-based ecosystem model predictions of carbon and water fluxes in

major European forest biomes. Global Change Biol. 11, 2211–2233.

Noilhan, J., Planton, S., 1989. A simple parameterization of land surface processes for meteorological models. Mon. Wea. Rev. 117, 536–549.

Noilhan, J., Mahfouf, J.-F., 1996. The ISBA land surface parameterisation scheme. Global Planetary Change 13, 145–159.

Oechel, W.C., Vourlitis, G.L., Hastings, S.J., Zulueta, R.C., Hinzman, L., Kane, D., 2000. Acclimation of ecosystem CO_2 exchange in the Alaskan Arctic in response to decadal climate warming. Nature 406, 978–981.

Papale, D., Reichstein, M., Aubinet, M., Canfora, E., Bernhofer, C., Kutsch, W., Longdoz, B., Rambal, S., Valentini, R., Vesala, T., Yakir, D., 2006. Towards a standardized processing of Net Ecosystem Exchange measured with eddy covariance technique: algorithms and uncertainty estimation. Biogeosciences 3, 571–583.

Parton, W.J., Schimel, D.S., Cole, C.V., Ojima, D.S., 1987. Analysis of factors controlling soil organic matter levels in Great Plains grasslands. Soil Sci. Soc. Am. J. 51, 1173–1179.

Pilegaard, K., Hummelshoej, P., Jensen, N.O., Chen, Z., 2001. Two years of continuous CO_2 eddy-flux measurements over a Danish beech forest. Agric. For. Meteorol. 107, 29–41.

Rannik, U., Altimir, N., Raittila, J., Suni, T., Gaman, A., Hussein, T., Holtta, T., Lassila, H., Latokartano, M., Lauri, A., Natsheh, A., Petaja, T., Sorjamaa, R., Yla-Mella, H., Keronen, P., Berninger, F., Vesala, T., Hari, P., Kulmala, M., 2002. Fluxes of carbon dioxide and water vapour over Scots pine forest and clearing. Agric. For. Meteorol. 111, 187–202.

Reichstein, M., Ciais, P., Papale, D., Valentini, R., Running, S., Viovy, N., Cramer, W., Granier, A., Ogée, J., Allard, V., Aubinet, M., Bernhofer, C., Buchmann, N., Carrara, A., Grünwald, T., Heimann, M., Heinesch, B., Knohl, A., Kutsch, W., Loustau, D., Manca, G., Matteucci, G., Miglietta, F., Ourcival, J., Pilegaard, K., Pumpanen, J., Rambal, S., Schaphoff, S., Seufert, G., Soussana, J.-F., Sanz, M.-J., Vesala, T., Zhao, M., 2007. Reduction of ecosystem productivity and respiration during the European summer 2003 climate anomaly: a joint flux tower, remote sensing and modelling analysis. Global Change Biol. 13, 634–651.

Rivalland, V., Calvet, J.-C., Berbigier, P., Brunet, Y., Granier, A., 2005. Transpiration and CO_2 fluxes of a pine forest: modelling the undergrowth effect. Ann. Geophysicae 23, 1–14.

Ruimy, A., Dedieu, G., Saugier, B., 1996. TURC: a diagnostic model of continental gross primary productivity and net primary productivity. Global Biogeochem. Cycles 10, 269–286.

Sarmiento, J., Gruber, N., 2002. Sinks for anthropogenic carbon. Phys. Today 55, 30–36.

Sellers, P.J., Randall, D.A., Collatz, G.J., Berry, J.A., Field, C.B., Dazlich, D.A., Zhang, C., Collelo, G.D., Bounoua, L., 1996. A revised land surface parameterization (SiB_2) for atmospheric GCMs. Part I: model formulation. J. Climate 9, 676–705.

Stöckli, R., Vidale, P.L., 2005. Modeling diurnal to seasonal water and heat exchanges at European FLUXNET sites. Theor. Appl. Climatol. 80, 229–243.

Sun, J., Burns, S.P., Delany, A.C., Oncley, S.P., Turnipseed, A.A., Stephens, B.B., Lenschow, D.H., LeMone, M.A., Monson, R.K., Anderson, D.E., 2007. CO_2 transport over complex terrain. Agric. For. Meteorol. 145, 1–21.

Twine, T.E., Kustas, W.P., Norman, J.M., Cook, D.R., Houser, P.R., Meyers, T.P., Prueger, J.H., Starks, P.J., Wesely, M.L., 2000. Correcting eddy-covariance flux underestimates over a grassland. Agric. For. Meteorol. 103, 279–300.

Valentini, R., Matteucci, G., Dolman, A.J., Schulze, E.-D., Rebmann, C., Moors, E.J., Granier, A., Gross, P., Jensen, N.O., Pilegaard, K., Lindroth, A., Grelle, A., Bernhofer, C., Grünwald, T., Aubinet, M., Ceulemans, R., Kowalski, A.S., Vesala, T., Rannik, U., Berbigier, P., Loustau, D., Gudmundsson, J., Thorgeirsson, H., Ibrom, A., Morgenstern, K., Clement, R., 2000. Respiration as the main determinant of carbon balance in European forests. Nature 404, 861–865.

Wilson, K.B., Baldocchi, D.D., 2000. Seasonal and interannual variability of energy fluxes over a broadleaved temperate deciduous forest in North America. Agric. For. Meteorol. 100, 1–18.

Wilson, K., Goldstein, A., Falge, E., Aubinet, M., Baldocchi, D., Berbigier, P., Bernhofer, C., Ceulemans, R., Dolman, H., Field, C., Grelle, A., Ibrom, A., Law, B.E., Kowalski, A., Meyers, T., Moncrieff, J., Monson, R., Oechel, W., Tenhunen, J., Valentini, R., Verma, S., 2002. Energy balance closure at FLUXNET sites. Agric. For. Meteorol. 113, 223–243.